

tion and, as such, would seem to be a definite possibility for representing the actual damage situation in fused silica. If it is further assumed that one or both of the *C* and *E* centers arise from a trapping of an electron or hole by the defects arising when an Si—O bond is broken, then the lack of correlation between the number of *C* and *E* centers remaining after a thermal anneal¹⁵ can be explained in terms of the trapping of charges by impurities. That is, impurities compete with the defects for the free charges. This also could explain the small *C*-band coloration and the presence of the additional absorption band at 257 m μ which appears to be associated with the hydroxyl-ion in the less pure silica (7940).

The broken-bond model requires strained regions so that the broken bond will relax quickly and not reform. This mechanism is probably not operative to any large extent in crystalline α quartz and could explain the relatively small damage observed in this material.

In terms of this broken-bond model one can under-

stand the reduced damage in fused silica when an anneal at 950°C precedes the irradiation. The strained regions already present in the glass would be relieved and would thus reduce the number of broken bonds formed as a result of irradiation. It is not clear, however, why there is decreased sensitivity when the sample in question has been irradiated prior to the 950°C anneal. It may be that the larger number of broken bonds allows greater freedom of re-arrangement of the lattice constituents than is possible during the anneal of the previously unirradiated material.

ACKNOWLEDGMENTS

The authors wish to acknowledge the assistance of James G. Allard in making the electron irradiations. F. H. Attix was especially helpful in discussions of dosimetry and the interactions of radiation with solids. They are also pleased to acknowledge the benefit gained from discussions with Dr. James H. Schulman, Dr. Clifford C. Klick, and Dr. David L. Dexter.

Test of Spin Hamiltonian for Iron³⁺ in Strontium Titanate

SOL AISENBERG AND H. STATZ, *Research Division, Raytheon Company, Waltham, Massachusetts*

AND

G. F. KOSTER, *Physics Department, Massachusetts Institute of Technology, Cambridge, Massachusetts*

(Received June 18, 1959)

The applicability of a conventional spin Hamiltonian to the paramagnetic spectrum of Fe³⁺ in strontium titanate is investigated. The work was inspired by a paper by Müller who finds deviations from a conventional spin Hamiltonian which he attributed to covalent bonding. The spectrum is remeasured and compared with the more general theory of Koster and Statz. It is found that the conventional Hamiltonian describes the spectrum about as well, in this case, as the improved theory. The remaining discrepancies vary from crystal to crystal and are due to random distortions of the Fe³⁺ site. A rather good agreement with theory was obtained for one crystal which apparently was more perfect than the other measured samples. From perturbation theory, it is concluded that the deviations from a conventional Hamiltonian should be about 0.1 Mc/sec if covalency and exchange effects can be neglected. The experimental errors in the present experiments are about 1 to 2 Mc/sec. Even though for the present example it is unnecessary to resort to the improved theory, it is shown that, even in the absence of covalency, measurable deviations from a conventional spin Hamiltonian are expected in substances where the zero-field splittings and the applied magnetic field are large.

I. INTRODUCTION

IN the literature, one sometimes finds statements that the spin Hamiltonian^{1,2} is not completely satisfactory in describing the energy levels of paramagnetic ions as a function of magnetic field. For example, in connection with maser studies, attention has been called again to the fact that gadolinium ethyl sulfate diluted in lanthanum ethyl sulfate shows a spectrum at low frequencies and lower temperatures not consistent

with a spin Hamiltonian.³ Müller stated in a recent paper⁴ that Fe³⁺ in strontium titanate showed deviations from a spin Hamiltonian. Geusic⁵ stated that he observed deviations from a spin Hamiltonian of the order of one percent for Cr³⁺ in Al₂O₃ crystals.

Observed deviations from spin Hamiltonian may have many reasons. First of all, the approximations underlying a spin Hamiltonian may introduce errors which are larger than the experimental uncertainties.

¹ B. Bleaney and K. W. H. Stevens, *Reports on Progress in Physics* (The Physical Society, London, 1953), Vol. 16, p. 108.

² K. D. Bowers and J. Owen, *Reports on Progress in Physics* (The Physical Society, London, 1955), Vol. 18, p. 304.

³ Bleaney, Scovil, and Trenam, *Proc. Roy. Soc. (London)* **A223**, 15 (1954).

⁴ K. A. Müller, *Helv. Phys. Acta* **31**, 173 (1958).

⁵ J. E. Geusic, *Phys. Rev.* **102**, 1252 (1956).

Also, the experimental observations may be in error. The symmetry of the lattice site may also be different from what is assumed. For example, when the paramagnetic ions are substituted into the host crystal the charge on the substituted ions, in general, will be different from those ions originally present at that site. To achieve over-all balance in charge, anion or cation vacancies may be created or other charge balancing defects must be present. These vacancies may be in the vicinity of the atom in question and distort the crystal symmetry. Also strains induced during the crystal growth cause deviations from the assumed symmetry.

Adding to possible discrepancies are calculational uncertainties. The energy levels of the spin Hamiltonian can be calculated by diagonalizing the Hamiltonian matrix. Some workers have determined these energy levels by perturbation theory rather than by an exact computing machine diagonalization and thus have obtained discrepancies between calculations and experiment. Finally there is the possibility that the lattice distorts around the paramagnetic ion as the magnetic field is applied. Such a distortion would follow the direction of the magnetic field. Measuring a cubic crystal, for example, would give a spectrum with cubic symmetry even though the symmetry of the lattice site would always deviate from cubic symmetry. Such a distortion could result from the magnetic field induced changes in the wave function of the paramagnetic ion and its interaction with neighboring atoms. Bleaney *et al.*³ invoked this concept as a possible explanation of the experimental observations in gadolinium ethyl sulfate.

In a first step, two of the authors investigated the applicability of the spin Hamiltonian.^{6,7} A new group theoretical method was developed in which it was assumed that we know the ground-state wave functions exactly. The magnetic field was introduced as a perturbation $\beta\mathbf{H}\cdot(\mathbf{L}+2\mathbf{S})$ and the Hamiltonian matrix for this perturbation for the lowest states was determined. Due to the transformation properties of the lowest states and due to time inversion symmetries there are many relations between these matrix elements. For a ${}^6\text{S}$ state in a cubic field, there remain only five independent matrix elements which may be considered as adjustable constants when fitting the experimental data to this theory. As will be shown, the remaining error in this new theory is entirely negligible and deviations still remaining must be attributed to such effects as distortions of the lattice in the vicinity of the atom due to either the Jahn-Teller effect, or defects, or other effects not contained in the deviation of the theory.

In order to see to which extent the conventional spin Hamiltonian theory applies and whether there are

any deviations from either the old or the improved theory, we have investigated as a first example Fe^{3+} in strontium titanate. We have chosen this material since Müller has reported deviations from a conventional spin Hamiltonian formalism for this crystal which he felt might have been due to covalent bonding. In the new theory, effects due to covalent bonding are included and thus a fit should be obtainable. We have preferred this crystal to gadolinium ethyl sulfate or ruby since the crystal structure is cubic and thus the number of available constants is still reasonably small. It will turn out, however, that the conventional spin Hamiltonian will describe the spectrum much better than believed and the small remaining discrepancies are not materially reduced by the new constants. The origin of the residual discrepancy will be shown to be due to noncubic fields splitting the quadruple zero field degeneracy (Γ_8^+) into two doubly degenerate levels.

II. EXPERIMENTAL PROCEDURE

The paramagnetic resonance spectrometer illustrated in Fig. 1 is used to measure the interaction of electromagnetic energy with paramagnetic spins in a magnetic field. It is similar to those described in the literature^{8,9} with the exception of a few modifications which are evident in the figure.

The magnetic field is modulated by about 1 gauss or less at 25 cycles per second, and the resulting signal which is proportional to $d\chi''/dH$ is measured with a specially designed, narrow band, phase sensitive detector. The low-noise preamplifier and phase-sensitive detector each have a tuned amplifier stage with a Q variable from 25 to zero. Two rejection filters are included in the preamplifier. The gain of the complete system is about 5×10^7 with full scale corresponding to an input of 0.2 microvolt to the transformer. The equivalent input noise is about 5×10^{-9} volt for a band width of 1 cps at a frequency of 25 cps. The output of the phase-sensitive detector can be used to keep the magnetic field locked to the center of an absorption line. This method is illustrated in Fig. 1. The time constant of this negative feedback loop is kept high (up to 500 seconds) in order to prevent oscillation at high amplifier gain and to reduce the effect of noise in the determination of the line center.

The microwave frequency is measured with a cavity wavemeter which is calibrated to an absolute accuracy of 1 Mc/sec, and which has a resolution of about 0.1 Mc/sec. Magnetic fields are measured with a nuclear resonance magnetometer and a 10 Mc/sec counter. Since the proton resonance probe is physically displaced from the paramagnetic sample, a slight correction (about 0.5 gauss) is made for the difference of field between the two points. When two resonance lines are not completely resolved, a correction must be made for

⁶ G. F. Koster and H. Statz, *Phys. Rev.* **113**, 445 (1959).

⁷ H. Statz and G. F. Koster (to be published).

⁸ Strandberg, Tinkham, Solt, and Davis, *Rev. Sci. Instr.* **27**, 596 (1956).

⁹ G. Feher, *Bell System Tech. J.* **36**, 449 (1957).

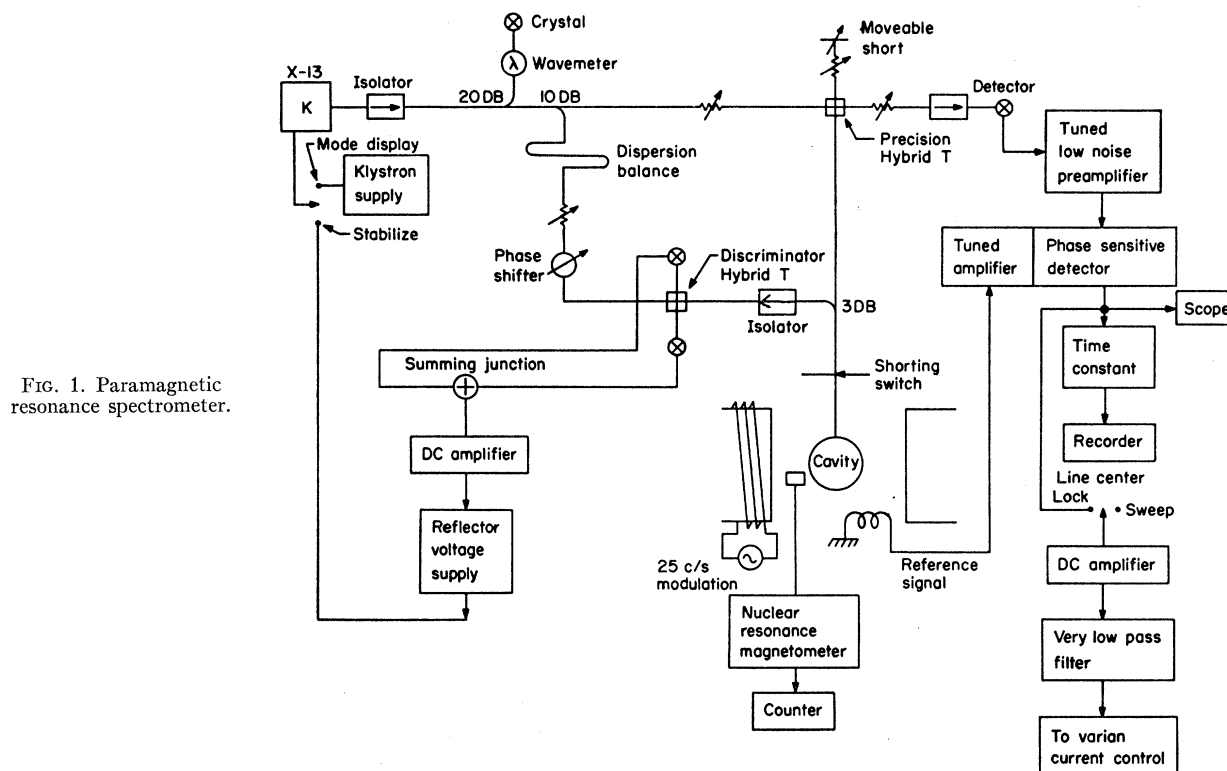


FIG. 1. Paramagnetic resonance spectrometer.

the "line interaction" effect which tends to make the apparent line centers slightly different from the values that correspond to the separate lines. If one can assume a Lorentz line shape, then the correction can be computed in terms of the apparent line separation, the linewidths, and the line amplitudes. The corrections are obtained from two fifth-order simultaneous equations which are solvable by successive approximations. The assumption of a Lorentz shape may be questioned when the lines overlap only in the wings. In that case, however, the line shift corrections are negligible and the detailed line shape is not significant. Larger corrections correspond to greater overlap; hence, the assumption of a Lorentz shape becomes more accurate and the values of the corrections are more accurate.

The samples were from single crystal boules of iron-doped SrTiO_3 and were in the form of thin disks with the $[110]$ direction parallel to the axis of the cylinder. The sample was mounted in a cylindrical resonant cavity operated in the TE_{101} mode, with the axis of the sample coincident with the axis of the cavity. The initial orientation of the sample was obtained by means of x-rays. The crystal can be rotated completely around the cylinder axis with a resolution of about 0.01 degree. Since the $[110]$ plane and the plane of rotation are not necessarily exactly identical, provision is made for a variable tilt angle with a range of a few degrees and a resolution of better than 0.01 degree. There is a simple method for making certain crystallographic directions

exactly parallel to the magnetic field. For the $[100]$, $[110]$, and $[111]$ directions the resonance field as a function of angle is an extremum, so that variation of the crystal orientation through small deviations about these directions will permit exact orientation of the crystal with respect to the magnetic field in these three directions. When the measurements were repeated to check the reproducibility of the results, the average agreement of the rotation angles was 0.11 degree; the average agreement of the tilt angles was 0.08 degree.

III. EXPERIMENTAL RESULTS

Table I lists the results of measurements at room temperature for a microwave frequency of about 10 kMc/sec. The five resonance lines for the Fe^{3+} ions are designated A , B , C , D , and E in the order of increasing field. The resonance field values corrected for the magnet gradient and the "line interaction" are listed along with the average deviations between repeated readings. The sample was cut from a boule containing 0.01 weight percent of iron.

The initial set of measurements was used for the comparison of theory with experiment. A second set of measurements on the identical sample was used for the experimental validation of the original measurements. When the second set was corrected (0.2 gauss or less) for the slight frequency difference between the sets, the deviations between sets were found to average 0.4 gauss. These deviations correspond to the composite

TABLE I. Measured and calculated line positions.

Direction type	Line	100 ppm original run		100 ppm repeat run	Linewidth $2\delta B$ gauss (c)	Calculated frequencies		
		f_0 Mc/sec	\bar{B}_0 gauss (a)	\bar{B}_0 gauss (b)		Müller's constant Mc/sec	Least squares fit with 5-parameter theory Mc/sec	Deviations of 5-parameter theory from original run Mc/sec
[100]	A	$10\,001.3 \pm 1.0$	3037.4 ± 0.1	3037.1 ± 0.2	15.2 ± 0.6	10 019.9	10 010.2	+8.9
	B		3140.6 ± 0.1	3140.4 ± 0.1	23.4 ± 1.2	9998.4	9989.0	-12.3
	C		3565.3 ± 0.2	3565.2 ± 0.1	8.8 ± 0.6	10 000.6	10 000.7	-0.6
	D		3990.4 ± 0.2	3990.7 ± 0.2	22.1 ± 0.7	10 003.5	10 010.9	+9.6
	E		4085.9 ± 0.1	4086.1 ± 0.1	14.1 ± 0.2	9983.2	9995.6	-5.7
[110]	A	$10\,000.5 \pm 1.0$	3424.5 ± 0.2	3424.6 ± 0.2	13.7 ± 0.5	10 007.6	10 004.0	+3.5
	B		3454.1 ± 0.2	3454.7 ± 0.2	16.1 ± 0.1	9997.2	9996.1	-4.4
	C		3572.2 ± 0.3	3572.6 ± 0.2	9.5 ± 0.2	9997.9	9999.8	-0.7
	D	
	E		3684.7 ± 0.2	3685.3 ± 0.2	11.9 ± 0.1	9995.6	9997.2	-3.3
[111]	A	$10\,001.2 \pm 1.0$	3225.2 ± 0.1	3224.8 ± 0.4	12.4 ± 0.3	10 009.1	10 003.3	+2.1
	B		3275.2 ± 0.1	3274.7 ± 0.3	12.8 ± 0.5	10 008.9	10 003.6	+2.4
	C		3547.4 ± 0.1	3547.1 ± 0.2	9.8 ± 0.3	10 003.0	10 001.1	-0.1
	D		3837.6 ± 0.1	3838.1 ± 0.3	12.8 ± 0.2	9995.2	10 001.5	+0.3
	E		3924.6 ± 0.2	3925.3 ± 0.4	11.9 ± 0.5	9993.1	10 001.8	+0.6

* Corrected for "line interaction" and field gradient.

b Measured at $10\,000.7 \pm 1.0$ Mc/sec and corrected to values corresponding to frequencies of original run (for $g \approx 2.0$: corrections range up to 0.2 gauss).

c Measured between turning points on the derivative trace.

d This line was not resolved.

TABLE II. Comparison of line positions of two crystals with different Fe^{3+} concentrations.

Direction type	Line	f_0 Mc/sec	100 ppm sample repeat run (Table I)		10 ppm sample		Line center shift gauss
			\bar{B}_0 gauss	Linewidth $2\delta B$ gauss	\bar{B}_0 gauss	Linewidth $2\delta B$ gauss	
[100]	A	$10\,000.7 \pm 1.0$	3036.9 ± 0.2	15.2 ± 0.6	3037.3 ± 0.4	24.0 ± 0.3	+0.4
	B		3140.2 ± 0.1	23.4 ± 1.2	3145.9 ± 0.3	52.8 ± 0.2	+5.7
	C		3565.0 ± 0.1	8.8 ± 0.6	3565.3 ± 0.1	10.3 ± 0.1	+0.3
	D		3990.5 ± 0.2	22.1 ± 0.7	3994.1 ± 1.0	40.3	+3.6
	E		4085.9 ± 0.1	14.1 ± 0.2	4085.8 ± 0.3	24.3 ± 1.7	-0.1

errors introduced by the line center determination, the magnetic field measurement, the independent determination of the crystal directions, and any possible drift in the wavemeter calibration. The linewidths are also measured a number of times and the average values are tabulated along with the average deviations of the various measurements. These linewidths correspond to the difference between the derivation maxima.

In order to determine the variation of the spectrum from boule to boule and the variation with iron doping, measurements were made for H in the [100] direction on SrTiO_3 containing 10 parts per million of iron. The results are surprising and are summarized in Table II. There is a definite increase in linewidth for the lower iron concentration. In addition, there is a definite

shift of line centers particularly for lines B and D , both of which have the largest increase in linewidth. The spins are so diluted that any exchange narrowing for the more concentrated sample is improbable. Apparently the past history of the boule preparation significantly influences the linewidth and line center. Essentially after completion of these measurements and calculations a sample containing 300 parts per million of iron was measured which was apparently more perfect than the other investigated samples. The results of the measurements are summarized in Table III.

IV. DETERMINATION OF THE CONSTANTS OF THE THEORY

As has been experimentally observed (Tables I, II, and III) there are, in the line position, variations which change from crystal to crystal. It is therefore impossible to ascribe too much significance to small deviations of experiment from theory. We shall, however, use the data of Table I to determine the constants of the 5 parameter theory.

As was shown in reference 6, the energy levels of a S state in a cubic environment are described by the solution of the following secular determinant:

TABLE III. Deviations between theory and experiment for 300 parts per million sample.

Line	Deviations (calc-exp) Mc/sec		
	[100]	[110]	[111]
A	+3.9	+2.5	+4.0
B	+0.6	+5.5	+3.7
C	+1.1	+3.6	+0.7
D	+1.0	...	+0.5
E	+3.3	+1.0	+1.1

$H_x\beta g_1 + \Delta E$	$\frac{\sqrt{3}}{4}$	0	$\frac{i}{4}$	$\frac{i}{2}$	$H_x\beta g_4$
$-E$	$-\frac{iH_y\beta(g_1+g_2)}{4}$	0	$-\frac{H_y\beta g_1 - \frac{3}{4}iH_y\beta g_2}{4}$	$-\frac{H_y\beta g_4}{2}$	0
$\frac{\sqrt{3}}{4}$	$-\frac{H_x\beta(g_1+g_2)}{4}$	0	$\frac{1}{4}H_x\beta g_1 - \frac{3}{4}H_x\beta g_2$	$\frac{1}{2}H_x\beta g_4$	0
$H_x\beta g_2 + \Delta E$	$\frac{\sqrt{3}}{4}$	0	$\frac{i}{4}$	0	$\frac{\sqrt{3}}{2}$
$-\frac{iH_y\beta(g_1+g_2)}{4}$	$-E$	$-\frac{3}{4}iH_y\beta g_1 - \frac{1}{4}H_y\beta g_2$	0	0	$-\frac{iH_y\beta g_4}{2}$
$\frac{\sqrt{3}}{4}$	$-\frac{H_x\beta(g_1+g_2)}{4}$	$\frac{3}{4}H_x\beta g_1 - \frac{1}{4}H_x\beta g_2$	0	0	$-\frac{\sqrt{3}}{2}H_x\beta g_4$
0	$\frac{3}{4}iH_y\beta g_1 - \frac{1}{4}H_y\beta g_2$	$-E$	$-\frac{\sqrt{3}}{4}$	$-\frac{\sqrt{3}}{2}$	0
$\frac{3}{4}H_x\beta g_1 - \frac{1}{4}H_x\beta g_2$	$-\frac{H_x\beta g_2 + \Delta E}{4}$	$-E$	$-\frac{iH_y\beta(g_1+g_2)}{4}$	$-\frac{iH_y\beta g_4}{2}$	0
$\frac{i}{4}$	$\frac{3i}{4}$	0	$\frac{\sqrt{3}}{4}$	$-\frac{\sqrt{3}}{2}$	0
$-\frac{H_y\beta g_1 + \frac{3}{4}H_y\beta g_2}{4}$	0	$-\frac{iH_y\beta(g_1+g_2)}{4}$	$-\frac{\sqrt{3}}{4}$	$-\frac{\sqrt{3}}{2}$	0
$\frac{1}{4}H_x\beta g_1 - \frac{3}{4}H_x\beta g_2$	0	$-\frac{H_x\beta g_2 + \Delta E}{4}$	$-\frac{iH_y\beta(g_1+g_2)}{4}$	$-\frac{iH_y\beta g_4}{2}$	0
$\frac{i}{2}$	0	$\frac{\sqrt{3}}{2}$	$-\frac{H_x\beta g_1 + \Delta E}{4}$	$H_x\beta g_4$	$\frac{i}{2}$
$-\frac{H_y\beta g_4}{2}$	0	$+\frac{iH_y\beta g_4}{2}$	$-E$	$H_x\beta g_4$	$-\frac{i}{2}H_y\beta g_4$
$\frac{1}{2}H_x\beta g_4$	0	$+\frac{\sqrt{3}}{2}H_x\beta g_4$	$-\frac{H_x\beta g_3}{2}$	$-E$	$iH_y\beta g_3$
$H_x\beta g_4$	$\frac{\sqrt{3}}{2}$	0	$\frac{i}{2}$	$-\frac{H_x\beta g_3}{2}$	$-\frac{H_x\beta g_3}{2}$
$+\frac{iH_y\beta g_4}{2}$	0	0	$-\frac{iH_y\beta g_4}{2}$	$-iH_y\beta g_3$	$H_x\beta g_3$
$-\frac{\sqrt{3}}{2}H_x\beta g_4$	0	0	$-\frac{1}{2}H_x\beta g_4$	$-H_x\beta g_3$	$-E$

(1)

The unknown constants are g_1, g_2, g_3, g_4 , and the zero-field splitting ΔE . The conventional spin Hamiltonian theory describes the energy levels of a 6S state as the solution of another secular determinant which results from

$$H_{\text{eff}} = g\beta\mathbf{H}\cdot\mathbf{S} + a(S_x^4 + S_y^4 + S_z^4) \quad (2)$$

acting between the six substates of a spin angular momentum $S = \frac{5}{2}$. The predictions of Eq. (2) are contained in the more general Matrix (1) as a special case. The five normally independent constants of Matrix (1) become related to the two constants of Eq. (2) in the following way:

$$g_1 = -(11/6)g; \quad g_2 = \frac{1}{2}g; \quad g_3 = \frac{5}{6}g; \\ g_4 = -\frac{2}{3}(5)^{\frac{1}{2}}g; \quad \Delta E = 18a. \quad (3)$$

The secular determinant (1) is, in general, complex. For machine diagonalization, the complex matrix has to be transformed into a real one. Denote the Hermitian Matrix (1) by \mathbf{H} . Then we may decompose it into its real and imaginary parts,

$$\mathbf{H} = \mathbf{H}_r + i\mathbf{H}_{im}. \quad (4)$$

The real symmetric matrix

$$\begin{pmatrix} \mathbf{H}_r & -\mathbf{H}_{im} \\ \mathbf{H}_{im} & \mathbf{H}_r \end{pmatrix} \quad (5)$$

can be shown to have the same eigenvalues as (4); however, each eigenvalue occurs twice as often as in (4). The dimension of the matrix has, however, also doubled which means an approximately eightfold

increase in computing time. In fitting the undetermined parameters of Matrix (1), many diagonalizations are required. For certain directions of H , symmetry considerations may be used to partly diagonalize the matrix. In the present case we want to fit the energy levels for H lying in the $[100]$, $[110]$, and $[111]$ direction. In the $[100]$ direction the matrix is already partly diagonalized giving two 2×2 and one 1×1 matrix and thus no machine calculations are required for this direction. For the $[110]$ direction H may be chosen to lie in the $z-x$ plane and the matrix will be real. For the $[111]$ direction the matrix is complex, yielding a 12×12 real matrix.

Let us thus investigate how symmetry properties may be used to factor the matrix when H points in the $[111]$ direction. With the magnetic field pointing along the $[111]$ direction, the wave functions must still be invariant under the operations of the group C_{3i} . As may be readily verified (see for example Table II of reference 7) the substates of an angular momentum of $\frac{5}{2}$ span a representation of C_{3i} which contains the one dimensional irreducible representations Γ_4^+ , Γ_5^+ , and Γ_6^+ each twice (notation as in reference 7).

Since just the individual m_s substates form representations for these one dimensional groups, our Hamiltonian Matrix (1) should yield three 2×2 equations when written down in a basis of substates which are

quantized along the $[111]$ direction. From the 6 substates used for the evaluation (1), 4 belong to Γ_3^+ and 2 to Γ_7^+ (reference 6). As the basis for Γ_3^+ we used the spin $\frac{3}{2}$ substates as quantized along the z direction. For Γ_7^+ we used the representation generated by the spin $\frac{1}{2}$ substates multiplied by the one-dimensional representation Γ_2^+ (notation as in reference 7). The 6 basis functions ψ_i quantized along the z direction can be transformed into a new set of basis functions φ_j which are quantized along the $[111]$ direction. If the φ 's and ψ 's are presented in the form of a row vector, then the transformation from the ψ 's to the φ 's is performed by the matrix

$$U = \begin{pmatrix} \mathbf{D}^{\frac{3}{2}}(\alpha, \beta, \gamma) & 0 \\ 0 & \mathbf{D}^{\frac{1}{2}}(\alpha, \beta, \gamma) \end{pmatrix}, \quad (6)$$

where the \mathbf{D} 's are given by Rose.¹⁰ α , β , and γ take on the values $\pi/4$, $\arccos 1/\sqrt{3}$, and $\pi/4$, respectively. In the new system of eigenfunctions the original Matrix (1) which we shall designate by \mathbf{M} will be transformed into the new matrix \mathbf{M}' by the relation

$$\mathbf{M}' = \mathbf{U}^{-1}\mathbf{M}\mathbf{U}. \quad (7)$$

\mathbf{M}' is partially diagonal and consists of the following three 2×2 matrices:

$$\begin{pmatrix} \frac{5}{6}H\beta g_1 + \frac{1}{2}H\beta g_2 + \Delta E - E & \frac{1}{6}H\beta g_1 - \frac{1}{2}H\beta g_2 - i\beta(\frac{1}{6}Hg_1 - \frac{1}{2}Hg_2) \\ \frac{1}{6}H\beta g_1 - \frac{1}{2}H\beta g_2 + i\beta(\frac{1}{6}Hg_1 - \frac{1}{2}Hg_2) & -\frac{5}{6}H\beta g_1 - \frac{1}{2}H\beta g_2 + \Delta E - E \end{pmatrix} \\ \begin{pmatrix} \frac{1}{2}H\beta g_1 - \frac{1}{2}H\beta g_2 + \Delta E - E & -iH\beta g_4 \\ +iH\beta g_4 & -H\beta g_3 - E \end{pmatrix} \\ \begin{pmatrix} -\frac{1}{2}H\beta g_1 + \frac{1}{2}H\beta g_2 + \Delta E - E & +iH\beta g_4 \\ -iH\beta g_4 & H\beta g_3 - E \end{pmatrix}. \quad (8)$$

A similar procedure shows that the 6×6 matrix describing the energy levels in the $[110]$ direction can be factored into two 3×3 matrices. In the following calculations, however, the 6×6 matrix was left as is, since the computing time was not too prohibitive.

We would like to fit the constants to the measurements in the $[100]$, $[110]$, and $[111]$ direction by something equivalent to a least-squares fit. For this purpose, we start with the two-parameter spin Hamiltonian as determined by Müller.⁴ In Table I we show

TABLE IV. Value of constants.

	g_1	g_2	g_3	g_4	$\frac{\Delta E}{\text{kMc/sec}}$
Equivalent to Müller Constants as determined by least-squares fit using new Hamiltonian	-3.6740	1.0020	1.6700	-2.9874	1.7850
Change in parts per million	-32	12	192	-30	-7235

the calculated and measured transition frequencies. We next expand the frequency difference between any of the pairs of levels listed in Table I in a Taylor series in δg_1 , δg_2 , δg_3 , δg_4 , and $\delta \Delta E$. Here δg_1 , for example, is the difference between g_1 necessary to fit the data and the value of g_1 given by Eq. (3) using the value of g as determined by Müller. For some particular transition between levels i and k we can then write

$$\nu_{ik} = \nu_{ik}^0 + a_{ik}\delta g_1 + b_{ik}\delta g_2 + c_{ik}\delta g_3 + d_{ik}\delta g_4 + e_{ik}\delta \Delta E + \dots \quad (9)$$

In Eq. (9), ν_{ik}^0 is the frequency difference as calculated from the conventional spin Hamiltonian using Müller's constants. The constants a_{ik} , b_{ik} , etc., may be obtained by differentiation or by use of the computer by changing g_1 in Matrix (1) by a small amount and observing the new ν_{ik} . We next compute $\sum_{ik} (\nu_{ik} - \nu)^2$ where ν is the

¹⁰ M. E. Rose, *Elementary Theory of Angular Momentum* (John Wiley & Sons, Inc., New York, 1957), pp. 62-75.

observed transition frequency. The sum over i and k is meant to include those states between which transitions are obtained. We make the sum $\sum_{ik} (\nu_{ik} - \nu)^2$ a minimum by choosing δg_1 , etc., such that the partial derivatives of the sum with respect to δg_1 , etc., vanish. We thus obtain the new computed frequency values for the transitions. These values are given in Table I. The new constants are given in Table IV.

V. DISCUSSION OF THE RESULTS

From Table I, it becomes evident that the theory cannot completely fit the analyzed experimental results. Especially in the $[100]$ directions, there are deviations of the order of 10 Mc/sec.

It is clear that our theory should explain the experimental observations to very close tolerances. To prove this, we show in Fig. 2 the splitting of a 6S state due to the various interactions. After diagonalization of the Matrix (1), the remaining error in the i th state can be estimated, using second order perturbation theory,⁷ to be

$$\Delta E = \sum_k \frac{|H_{ik}|^2}{E_i - E_k} \quad (10)$$

H_{ik} is the matrix element to be taken with respect to the perturbing operator $g\beta\mathbf{H} \cdot (\mathbf{L} + 2\mathbf{S})$ between one of the lowest states (i) and any of the higher states (k). H_{ik} is only different from zero because the higher states, for example, the ${}^4T_{1g}$ states have admixtures from the 6S ground state due to the spin orbit coupling $L \cdot S$ or other interactions. The amount of the admixture is given by first order perturbation theory as

$$\frac{\langle {}^6S | \mathbf{L} \cdot \mathbf{S} | {}^4T_{1g} \rangle}{E({}^6S) - E({}^4T_{1g})}$$

The matrix element $\langle {}^6S | \mathbf{L} \cdot \mathbf{S} | {}^4T_{1g} \rangle$ may be estimated to be less than 1000 cm^{-1} . From Fig. 2, the smallest separation $E({}^6S) - E({}^4T_{1g})$ is approximately $20\,000 \text{ cm}^{-1}$. The matrix elements with respect to the perturbation $\beta\mathbf{H} \cdot (\mathbf{L} + 2\mathbf{S})$ between the sublevels of the 6S state are of the order of the splitting of the ground state due to the magnetic field, i.e., about 0.3 cm^{-1} . We thus arrive at a probable error in Eq. (10) of approximately 10^{-8} cm^{-1} . This is the contribution from one typical set of states and the summation over all states has to be carried out. It is, however, quite safe to conclude that the observed discrepancies of about $3 \times 10^{-4} \text{ cm}^{-1}$ cannot be explained by deficiencies in the theoretical model.

To explain the deviations of the theory from the experiment we shall consider the line widths of the various lines and the measurements that have been done on the sample marked by "10 parts per million." In Table I, we see that there is an indicated relationship between measured line widths and the deviation from the theory. In particular, we see that the lines marked

B and D for H in the $[100]$ direction have the largest linewidth and also the largest deviation from the least-square fit. We find that for the lower concentration sample marked 10 parts per million, the line widths are larger than in the higher concentration sample. The lines B and D for H in the $[100]$ direction are broadened most and also their centers shift by 5.7 and 3.6 gauss, respectively, from the values measured in the concentrated sample. These observations are indicative of a random distortion of the Fe^{3+} lattice sites. Such a random distortion shifts the lines of the individual atoms in a random manner. If the shifts are not linear in the amplitudes of the distortion than a net shift in the peak of the absorption line also results. Apparently the position of the lines B and D for H in the $[100]$ direction is affected most by the distortion. For the less concentrated sample we conclude from the linewidth that the random distortion causes shifts of the lines B and D for H in the $[100]$ direction of the order of 50 gauss for the individual atoms while the shift in the line center is about one order of magnitude smaller. Since the shift in the lines differs in the two samples, we conclude that it is not the Jahn-Teller effect which causes the distortion. Annealing of the sample marked 100 parts per million at 1400°C for 10 hours reduced the maximum deviations from 12.3 to 7.1 Mc/sec. As a final check on the conclusions to be obtained in this paper a sample containing 300 parts per million of iron was measured. Apparently it is the most perfect sample since the deviations from the least-square fit are almost within experimental error (Table III). A new least-square fit to the new data would make the deviations even smaller. Deviations of theory from experiment are thus due to sample imperfections which

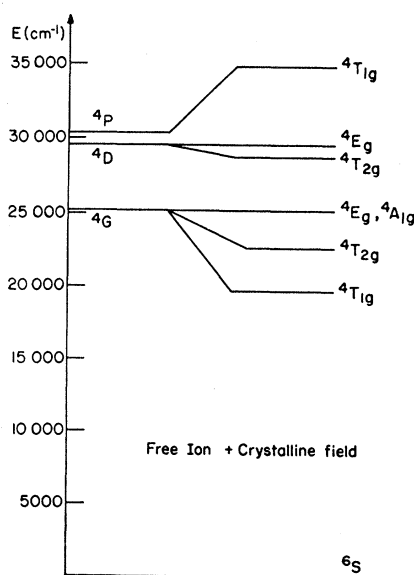


FIG. 2. Typical level arrangement of a $(d)^5$ configuration in a cubic field.

most probably consist of strains introduced in the growing process. The observed discrepancies are not likely to be due to charge neutralizing defects since their contribution is not expected to vary greatly from crystal to crystal.

Let us next consider the values of the new constants (Table IV). The largest correction occurs in the value of the zero-field splitting. The corrections in g_1 , g_2 , g_3 , and g_4 are relatively small and probably inside the experimental error. In the conventional spin Hamiltonian all g 's are related. In the more general theory the various g 's are independent of each other. In the present case the deviations from the g values as derived from a conventional spin Hamiltonian are small and comparable to the experimental error so that we cannot attribute significance to them.

It is interesting to note that in the present case the additional parameters of the new theory are too small to be detected. We therefore believe that the deviations which have been observed by Müller are not due to covalent bonding effects not included in the two-parameter Hamiltonian, but rather are due to distortions of the Fe^{3+} lattice sites.

Let us now compare these experimental results with the predictions of conventional perturbation theory which neglects effects due to covalent bonding and exchange. We investigate in which order of perturbation theory we first obtain terms not describable by a two-parameter spin Hamiltonian. This is done by considering as a perturbation on the atomic energy levels the cubic field, spin-orbit, and spin-spin interactions, and the Zeeman energy. In a given order of perturbation theory, the shift in energy is then given by products of matrix elements of these various perturbations divided by energy denominators of the order of magnitude of the multiplet separations ($\approx 20\,000\text{ cm}^{-1}$). It is easily shown that for each chain of matrix elements¹¹ which contributes to the zero-field splitting there is in the next order of perturbation theory a corresponding chain

involving one more matrix element, namely one of $\beta\mathbf{H}\cdot(\mathbf{L}+2\mathbf{S})$ between the 6S substates. These matrix elements give rise to a discrepancy with the two-parameter spin Hamiltonian. We have not found as yet matrix elements which give discrepancies in the same order of perturbation theory where the zero-field splitting terms appear. We could, however, prove that such terms do not exist when we neglect spin-spin and, of course, covalency effects. If we always have to go to higher order perturbation theory then the deviations from a conventional spin Hamiltonian may be estimated to be

$$\frac{(\text{zero-field splitting}) \times (\text{Zeeman energy})}{(\text{multiplet separation})}$$

Inserting the appropriate numbers for the present example we obtain about 0.1 Mc/sec. This is about ten times smaller than the experimental error. We see from this simplified estimate that measurable deviations are even expected if we neglect covalency, exchange, and similar effects in crystals which show large zero-field splittings and where high magnetic fields are employed (millimeter paramagnetic resonance measurements). As typical crystals, we may mention Fe^{3+} in MgWO_4 ¹² and Cr^{3+} in emerald.¹³ We may also expect the more complete Hamiltonian to be of importance where the crystalline field is very large as compared to the central field. Extreme cases of this type may occur when electrons are situated in lattice vacancies and other similar defects.

ACKNOWLEDGMENTS

Thanks are due Dr. O. Guentert and R. Mozzi for the x-ray orientation of the samples, and to Miss B. Healey for her help in the collection and processing of the data. We also wish to thank Miss W. Doherty for her help in the numerical computations.

¹² M. Peter, *Phys. Rev.* **113**, 801 (1959).

¹³ Geusic, Peter, and Schulz-Du Bois, *Bell System Tech. J.* **38**, 291 (1959).

¹¹ See H. Watanabe, *Progr. Theoret. Phys. (Kyoto)* **18**, 405 (1957), for many examples of such chains.